

1 Pathogen evasion of chemokine response through 2 suppression of CXCL10

3
4 Alejandro L. Antonia¹, Kyle D. Gibbs¹, Esme Trahair¹, Kelly J. Pittman¹, Benjamin H.
5 Schott¹, Jeffrey S. Smith², Sudarshan Rajagopal^{2,3}, J. Will Thompson⁴, R. Lee
6 Reinhardt^{5,6}, Dennis C. Ko^{1,7,8}

8 Affiliations

9 ¹Department of Molecular Genetics and Microbiology, School of Medicine, Duke
10 University, Durham, NC 27710

11 ²Department of Biochemistry, School of Medicine, Duke University, Durham, NC 27710

12 ³Division of Cardiology, Department of Medicine, School of Medicine, Duke University,
13 Durham, NC 27710

14 ⁴Proteomics and Metabolomics Shared Resource, Center for Genomics & Computational
15 Biology, School of Medicine, Duke University, Durham, NC 27710

16 ⁵Department of Biomedical Research, National Jewish Health, Denver, CO 27710

17 ⁶Department of Immunology and Microbiology, University of Colorado Anschutz Medical
18 Campus, Aurora, CO 80045

19 ⁷Division of Infectious Diseases, Department of Medicine, School of Medicine, Duke
20 University, Durham, NC 27710

21 ⁸Lead contact

22 *To whom correspondence should be addressed: Dennis C. Ko, 0048B CARL Building
23 Box 3053, 213 Research Drive, Durham, NC 27710. 919-684-5834.
24 dennis.ko@duke.edu. @denniskoHiHOST

25 **Abstract**

26 Clearance of intracellular pathogens, such as *Leishmania (L.) major*, depends on
27 an immune response with well-regulated cytokine signaling. Here we describe a
28 pathogen-mediated mechanism of evading CXCL10, a chemokine with diverse
29 antimicrobial functions, including T cell recruitment. Infection with *L. major* in a human
30 monocyte cell line induced robust *CXCL10* transcription without increasing extracellular
31 CXCL10 protein concentrations. We found that this transcriptionally independent
32 suppression of CXCL10 is mediated by the virulence factor and protease, glycoprotein-
33 63 (*gp63*). Specifically, GP63 cleaves CXCL10 after amino acid A81 at the base of a C-
34 terminal alpha-helix. Cytokine cleavage by GP63 demonstrated specificity, as GP63
35 cleaved CXCL10 and its homologues, which all bind the CXCR3 receptor, but not distantly
36 related chemokines, such as CXCL8 and CCL22. Further characterization demonstrated
37 that CXCL10 cleavage activity by GP63 was produced by both extracellular
38 promastigotes and intracellular amastigotes. Crucially, CXCL10 cleavage impaired T cell
39 chemotaxis *in vitro*, indicating that cleaved CXCL10 cannot signal through CXCR3.
40 Ultimately, we propose CXCL10 suppression is a convergent mechanism of immune
41 evasion, as *Salmonella enterica* and *Chlamydia trachomatis* also suppress CXCL10. This
42 commonality suggests that counteracting CXCL10 suppression may provide a
43 generalizable therapeutic strategy against intracellular pathogens.

44

45 **Keywords:** CXCL10; IP-10; leishmaniasis; Leishmania; gp63; leishmanolysin; T cell;
46 CXCR3; Chlamydia; Salmonella; convergent evolution

47 **Importance**

48 Leishmaniasis, an infectious disease that annually affects over one million people,
49 is caused by intracellular parasites that have evolved to evade the host's attempts to
50 eliminate the parasite. Cutaneous leishmaniasis results in disfiguring skin lesions if the
51 host immune system does not appropriately respond to infection. A family of molecules
52 called chemokines coordinate recruitment of the immune cells required to eliminate
53 infection. Here, we demonstrate a novel mechanism that *Leishmania (L.) major* employs
54 to suppress host chemokines: an *L. major* protease cleaves chemokines known to recruit
55 T cells that fight off infection. We observe that other common human intracellular
56 pathogens, including *Chlamydia trachomatis* and *Salmonella enterica*, reduce levels of
57 the same chemokines, suggesting a strong selective pressure to avoid this component of
58 the immune response. Our study provides new insights into how intracellular pathogens
59 interact with the host immune response to enhance pathogen survival.

60 **Introduction**

61 Proper immune clearance of intracellular pathogens requires precise cytokine and
62 chemokine signaling. These cytokines coordinate the localization, activation, and
63 polarization of innate and adaptive immune cell subsets. To study T cell recruitment and
64 polarization in response to intracellular pathogens, parasites in the genus *Leishmania*
65 have served as a paradigm (1). However, persistent gaps in the understanding of host
66 and pathogen factors that influence T cell response and recruitment contribute to the
67 dearth of immunotherapeutics and vaccines. With no available vaccine and limited
68 treatment options, *Leishmania* spp. continue to cause 1.2 million cases of cutaneous
69 leishmaniasis (CL) and 0.4 million cases of visceral leishmaniasis annually (VL) (2). A

70 better understanding of host immunity and pathogen evasion strategies is imperative to
71 develop alternative approaches to current therapies, which are limited by variable
72 efficacy, high cost, and growing drug resistance (3). Of particular relevance may be
73 instances where multiple diverse pathogens have evolved to evade or suppress the same
74 key host immune signaling pathways (4, 5).

75 To clear *L. major* parasites, a causative agent of CL, the adaptive immune system
76 must be coordinated to a type-1 response by appropriately recruiting immune cell
77 subsets, particularly CD4+ T helper 1 (T_h1) cells and CD8+ cytotoxic T lymphocytes
78 (CTLs) (6). This recruitment is mediated by chemokines, a family of signaling molecules
79 that regulate recruitment and localization of unique immune cell subsets. For example,
80 T_h1 cells, which mediate a pro-inflammatory response effective at eliminating intracellular
81 parasites, are recruited by chemokines such as CXCL10 through the CXCR3 receptor.
82 By contrast, T_h2 cells, which promote immunity targeting extracellular parasites, are
83 recruited by chemokines such as CCL22 through the CCR4 receptor (7). When infected
84 with *L. major*, T_h2 responding mice develop non-healing lesions, whereas T_h1 responding
85 mice effectively clear the parasite (8-10). As part of the broader type-1 immune response
86 against *L. major* infection, parasite-specific CD8+ cells are also recruited, and have been
87 implicated in productive immunity to primary and secondary infection (11-14).
88 Corresponding observational studies in humans support this model where non-healing
89 cutaneous lesions are characterized by T_h2 associated cytokines, and individuals
90 resistant to lesion development have a higher predominance of T_h1 associated cytokines
91 (15-18). Together these studies highlight the critical role of cytokine and chemokine
92 signaling in specific immune cell subsets during infection.

93 One of the chemokines that specifically regulates localization and activity of CD4+
94 T_h1 and effector CD8+ T-cells is CXCL10, or IFN γ Inducible Protein 10 (IP10). CXCL10
95 is part of a family of highly homologous chemokines, including CXCL9 and CXCL11,
96 which bind to and activate the CXCR3 chemokine receptor (reviewed in (19)). Multiple
97 lines of investigation suggest that CXCL10 protects against *Leishmania* infection. First,
98 the host upregulates *CXCL10* transcription throughout infection (20-22) and cells
99 expressing CXCR3 are expanded after infection (23). Second, BALB/c mice, which are
100 unable to control *Leishmania* spp. infection, demonstrate a defect in CXCR3 upregulation
101 (24, 25). Finally, exogenous CXCL10 is protective against both cutaneous and visceral
102 leishmaniasis (26-29). Therefore, the type-1 associated chemokine CXCL10 is important
103 for host control of cutaneous leishmaniasis.

104 Beyond *Leishmania*, type-1 immunity and CXCL10-CXCR3 signaling are critical
105 for clearing other intracellular pathogens. For the obligate intracellular bacterium
106 *Chlamydia trachomatis*, T_h1 cells are required for clearance of infection while a T_h2
107 dominated response may lead to excessive pathology (30-33). In mice, CXCL10 mRNA
108 and protein are significantly induced after infection (34-36). Similarly, T_h1 responses are
109 crucial for an effective immune response to the facultative intracellular bacteria
110 *Salmonella enterica* serovar Typhimurium based on studies in mice (37, 38) and the
111 predisposition of people with rare mutations in T_h1-promoting cytokines (IFN γ and IL12)
112 to invasive Salmonellosis (39). Further, M1-polarized macrophages, which restrict
113 *Salmonella* intracellular replication (40, 41), robustly upregulate *CXCL10* transcription
114 (42, 43). Finally, mice deficient for CXCR3 have increased susceptibility to *S. enterica*
115 (44), *Toxoplasma (T.) gondii* (45), and *C. trachomatis* (46). Thus, the CXCL10-CXCR3

116 signaling axis coordinates an adaptive type-1 immune response to intracellular pathogens
117 that promotes a successful healing response.

118 Here, we report that *L. major* suppresses extracellular CXCL10 protein levels,
119 providing a potential mechanism for evasion of the adaptive immune response. This
120 suppression occurs through the proteolytic activity of the virulence factor glycoprotein-63
121 (GP63). GP63 cleavage of CXCL10 occurs throughout *in vitro* infection and abrogates
122 CXCR3-dependent T cell migration. Furthermore, we observed CXCL10 suppression with
123 other intracellular pathogens, including *S. enterica* and *C. trachomatis*, demonstrating that
124 diverse intracellular pathogens have developed convergent mechanisms to suppress
125 CXCL10.

126

127 **Results**

128 ***L. major* infection suppresses CXCL10 protein, despite induction of CXCL10**
129 **mRNA.**

130 To broadly screen for *L. major* manipulation of host immunity, we measured
131 secreted levels of 41 cytokines following infection of lymphoblastoid cell lines (LCLs) with
132 *L. major*. LCLs constitutively produce CXCL10, and incubation with *L. major* reduced
133 CXCL10 levels by greater than 90% (Fig. 1A). We confirmed this decrease in CXCL10
134 protein in LPS-stimulated human THP-1 monocytes infected with *L. major* (Fig. 1B).
135 Despite the reduction in CXCL10 protein in culture supernatants, THP-1s exposed to *L.*
136 *major* had 2.5-fold higher CXCL10 mRNA relative to uninfected (Fig. 1B). Therefore, *L.*
137 *major* suppresses CXCL10 protein through a transcriptionally independent mechanism.

138 **The *L. major* matrix-metalloprotease, glycoprotein-63 (GP63), is necessary and**
139 **sufficient for CXCL10 protein suppression.**

140 To test whether an *L. major*-secreted factor is responsible for CXCL10 protein
141 suppression, we treated recombinant human CXCL10 with cell-free conditioned media
142 obtained from cultured *L. major* promastigotes. Again, CXCL10 was reduced by 90% with
143 the conditioned media (Fig. 2A). These results were consistent with proteolytic
144 degradation by a pathogen-secreted protease. We hypothesized that CXCL10
145 suppression was mediated by glycoprotein-63 (GP63), a zinc-metalloprotease conserved
146 among the *Trypanosoma* family of parasites and expressed in both the extracellular
147 promastigote and intracellular amastigote life stages (47-50). To test if GP63 is required
148 to suppress CXCL10, we used a known GP63 inhibitor, the zinc-chelator 1,10-
149 phenanthroline (51). 1,10-phenanthroline inhibited CXCL10-suppressive activity in *L.*
150 *major* conditioned media (Fig. 2A). Consistent with GP63-mediated degradation of
151 CXCL10, conditioned media from a promastigote culture of *L. major* deficient for *gp63*
152 ($\Delta gp63$; (52)) did not suppress CXCL10, whereas complementation with a single copy of
153 *gp63* (*L. major* $\Delta gp63+1$) restored CXCL10 suppression (Fig. 2B). Furthermore,
154 heterologously expressed GP63 secreted from mammalian HEK293T cells was sufficient
155 for complete CXCL10 suppression, while a single point mutation in the catalytic site of
156 GP63 (E265A) abrogated suppression (Fig. 2C). Therefore, GP63 is both necessary and
157 sufficient for CXCL10 suppression by *L. major*.

158 **GP63 selectively cleaves the CXCL10-related family of chemokines at the start of**
159 **the C-terminal alpha-helix.**

160 As GP63 has a diverse set of identified *in vitro* substrates (48), we examined the
161 specificity of GP63 across a spectrum of chemokines. Based on the initial cytokine screen
162 (Figure 1A), we hypothesized GP63 cleavage would be restricted to CXCL10 and highly
163 related chemokines. To experimentally test for GP63 cleavage, purified recombinant
164 chemokines were incubated with conditioned media from *L. major* WT, *L. major* $\Delta gp63$,
165 or *L. major* $\Delta gp63+1$. GP63 cleavage was observed for CXCL9 (38.14% amino acid
166 identity with CXCL10) and CXCL11 (30.85% amino acid identity with CXCL10) (Figure
167 3A, B), which both signal through CXCR3. By contrast, no cleavage of CXCL8 (IL-8; a
168 neutrophil-attracting chemokine) or CCL22 (MDC; a Th2-attracting chemokine) was
169 detected (Fig. 3B). Thus, chemokine cleavage by GP63 appears to preferentially degrade
170 chemokines involved in CXCR3 signaling.

171 Although western blot analysis supported GP63-dependent cleavage through loss
172 of CXCL10 immunoreactivity, it did not reveal the cleavage site or potential cleavage
173 products. The GP63 consensus cleavage site has been described as polar, hydrophobic,
174 and basic amino acids at positions P1, P1', and P2' (53). Following this pattern, there are
175 three potential cleavage sites in the mature CXCL10 protein (from amino acid position
176 22-96) that are conserved between human and murine CXCL10 (68.37% amino acid
177 identity) (Fig. 3A). In order to characterize the cleavage product(s), we incubated GP63
178 with human recombinant CXCL10 and visualized a shift in size by total protein stain (Fig.
179 3C). Intact CXCL10 and the largest cleavage products were determined to be 8.8kD and
180 6.6kD respectively, by capillary electrophoresis-mass spectrometry (CE-MS) (Fig. 3D).
181 After running the sample on a PAGE gel, the 8.8kD (intact, "Hi") product, 6.6kD (cleaved,
182 "Lo") product, and an uncleaved control ("Ctrl") were sequenced by trypsin digestion

183 followed by liquid chromatography-tandem mass spectrometry (LC-MS/MS). Comparison
184 of peptides after trypsin digest revealed a peptide from amino acids (AA) 74-81 that was
185 exclusively present in the cleaved CXCL10 band, but notably absent in the uncleaved
186 band (Fig. 3E). Conversely, distal peptide fragments such as AA84-91 were only present
187 in the uncleaved CXCL10. This analysis demonstrated cleavage occurring in between
188 A81 and I82, resulting in the loss of detectable peptides beyond those amino acids in
189 cleaved CXCL10. This is consistent with the fragment size based on intact molecular
190 weight CE-MS, and notably AIK (AA 81-83) is one of the three potential cleavage sites
191 identified in our comparative analysis (see Figure 3A). To confirm this site as preferred
192 for GP63 cleavage, we used site-direct mutagenesis to mutate the residues in the
193 proposed cleavage motif. Mutation of the identified P1 residue significantly slowed
194 CXCL10 cleavage in a time course experiment (Fig. 3F). Mapping the residues onto the
195 crystal structure of CXCL10 (54) demonstrated that cleavage occurs at the beginning of
196 the C-terminal alpha-helix of CXCL10 (Fig. 3G).

197 **GP63 produced by *L. major* promastigotes or amastigotes can cleave CXCL10**
198 **protein.**

199 Immediately after injection by the sand-fly vector, *Leishmania* parasites exist as an
200 extracellular, flagellated promastigote but are rapidly phagocytized where they transform
201 into the intracellular, aflagellated amastigote parasite stage. We hypothesized that GP63
202 would continue to be able to suppress CXCL10 through both stages of infection, as
203 transcriptomics indicate GP63 expression during both stages (50). To test the capacity of
204 *L. major* to suppress CXCL10 in both the promastigote and amastigote stage of infection,
205 we utilized PMA differentiated THP-1 monocytes as an intracellular macrophage model

206 of infection. Differentiated THP-1 monocytes were infected at an MOI of 20 with
207 promastigotes from *L. major* WT, $\Delta gp63$, or $\Delta gp63+1$. Extracellular promastigote activity
208 was assessed in the supernatant at 24 hours post infection, followed immediately by
209 washing to remove the extracellular promastigotes and GP63 protein in the media, and
210 subsequently assessing intracellular amastigote activity at 48 hours post infection.

211 This model demonstrated CXCL10 protein suppression by GP63 in both stages of
212 the parasite life cycle. *L. major* WT promastigotes had no induction of CXCL10 protein
213 relative to uninfected cells, while *L. major* $\Delta gp63$ infection resulted in a significant
214 induction of CXCL10 protein (Fig. 4A). Similarly, the *L. major* WT amastigotes continued
215 to suppress CXCL10 protein while *L. major* $\Delta gp63$ infection significantly induced CXCL10
216 protein (Fig. 4B). The complementation observed with the *L. major* $\Delta gp63+1$ strain is
217 significant, though incomplete in the promastigote stage and further reduced in the
218 amastigote stage. This is attributable to the plasmid construct being designed for high
219 expression in the promastigote stage (55) and the lack of G418 selection during the
220 experiment. Notably, all three *L. major* strains cause comparable induction of *CXCL10*
221 mRNA (Fig. 4C). These results indicate that CXCL10 mRNA is induced during
222 *Leishmania* infection, but protein levels are reduced by GP63, present at both parasite
223 life cycle stages involved in infection in mammalian hosts.

224 **GP63 cleaved CXCL10 is unable to recruit CXCR3 expressing T cells.**

225 Because CXCL10 coordinates the recruitment of CXCR3⁺ T cells during infection,
226 we next tested if GP63 cleavage of CXCL10 impacts T cell recruitment. We tested the
227 chemotactic ability of cleaved CXCL10 to recruit Jurkat T cells expressing CXCR3. The
228 basal chamber of a transwell system was seeded with CXCL10 in the presence of

229 conditioned media from *L. major* WT, *L. major* Δ gp63, or *L. major* Δ gp63+1. Conditioned
230 media from *L. major* WT and *L. major* Δ gp63+1 abrogated CXCL10 induced migration of
231 CXCR3+ Jurkat T cells, whereas the *L. major* Δ gp63 conditioned media did not impair
232 chemotaxis (Fig. 4D). Together these data support a model whereby the host attempts to
233 produce CXCL10 to coordinate recruitment of CXCR3 expressing immune cells, but *L.*
234 *major* produces GP63 to inactivate CXCL10 and impair T cell chemotaxis (Fig. 4E).

235 **CXCL10 suppression has evolved independently in multiple intracellular** 236 **pathogens**

237 Given that CXCL10 mediates a type-1 immune response that protects against a
238 broad range of intracellular pathogens, we asked if suppression of CXCL10 has evolved
239 in has evolved in other parasites and bacteria. CXCL10 production by LCLs was
240 measured by ELISA after exposure to a variety of pathogens including *Toxoplasma* (*T.*)
241 *gondii*, *Plasmodium* (*P.*) *bergei*, *Salmonella* (*S.*) *enterica* serovar Typhimurium,
242 *Chlamydia* (*C.*) *trachomatis*, *Mycobacterium* (*M.*) *marinum*, *Mycobacterium* (*M.*)
243 *smegmatis*, *Staphylococcus* (*S.*) *aureus*, and *Cryptococcus* (*C.*) *neoformans*. CXCL10
244 suppression of at least 80% was observed with two additional intracellular pathogens: *S.*
245 Typhimurium and *C. trachomatis*. In contrast, other pathogens, including the extracellular
246 pathogens *S. aureus* and *C. neoformans*, exhibited modest to no suppression of CXCL10
247 (Fig. 5A).

248 Confirmation and characterization of CXCL10 suppression in different cell lines
249 demonstrated that diverse intracellular pathogens impair chemokine accumulation. Using
250 a second LCL, we confirmed that *S. Typhimurium* and *C. trachomatis* infection suppress
251 CXCL10 (Fig. 5B-C). We then assessed the generalizability of CXCL10 suppression in

252 host cell types known to be commonly infected by each pathogen. THP-1 monocytes
253 stimulated with LPS upregulate significant production of CXCL10 protein, but infection
254 with live *S. Typhimurium* dramatically impaired this CXCL10 induction (Fig. 5D). Similarly,
255 the cervical epithelial cell line A2EN produces CXCL10 at baseline, but this is significantly
256 reduced after infection with *C. trachomatis* (Fig. 5E). Thus, multiple intracellular
257 pathogens that pose significant health burdens around the globe have independently
258 evolved the ability to suppress CXCL10 in the cell types relevant to their infective niche.

259

260 **Discussion**

261 We describe a mechanism used by intracellular pathogens to evade host
262 chemokine response. Specifically, *L. major* can significantly reduce CXCL10 and impair
263 its chemotactic activity through the matrix-metalloprotease, GP63. This strategy is likely
264 to be highly beneficial to the parasite as CXCL10 protects against *L. major* (29), *L.*
265 *amazonensis* (26), and *L. donovani* infection (27, 28). A similar phenotype of immune
266 evasion that is shared by diverse intracellular pathogens points to a critical conserved
267 role for CXCL10 in immunity to intracellular pathogens.

268 Consistent with CXCL10 playing a protective role during infection, multiple studies
269 show that recruitment of CXCR3-expressing cells actively shapes the immune response.
270 In response to *Leishmania* spp. specifically, CXCL10 is critical for the recruitment and
271 activation of several cell types that contribute to the coordination of a protective type-1
272 immune response: natural killer (NK) cells, CD8+ T cells, dendritic cells, and CD4+ T_h1
273 cells. With the early upregulation of *CXCL10* transcript (22), NK cells recruited during
274 infection produce IFN γ that contributes to T_h1 differentiation (29, 56). Specific subsets of

275 effector CD8+ T cells are recruited by CXCL10 after infection (23, 57). Finally, dendritic
276 cells exposed to CXCL10 produce increased IL12, a cytokine that promotes T_h1
277 polarization, and T_h1 cells exposed to CXCL10 produce greater amounts of IFN γ (58), a
278 signal which infected macrophages require for efficient parasite killing (6). Beyond
279 *Leishmania*, CXCR3-expressing cells have also been reported to play important roles in
280 other infectious and inflammatory models (19, 23, 59-62). After infection with lymphocytic
281 choriomeningitis virus, CXCR3 deletion leads to impaired production and localization of
282 effector CD8+ T cells (63), and CXCL10 precisely coordinates effector CD8+ T cells to
283 the site of *Toxoplasma gondii*, another intracellular eukaryotic pathogen (64). In response
284 to the bacterial pathogen *S. Typhimurium*, which we identified as also suppressing
285 CXCL10, mice have a significant expansion of CXCR3+ T_h1 cells which border bacteria-
286 rich granulomas in the spleen (43). These diverse examples highlight the importance of
287 evading the CXCL10-CXCR3 signaling axis for pathogens.

288 Current limitations of parasite genetics as they relate to the complexity of GP63
289 related proteases may contribute to an incomplete picture of the impact of GP63 on
290 chemokine suppression. First, sequencing *L. major* revealed proteins distantly
291 homologous to GP63 (approximately 35% amino acid identity) on chromosomes 24 and
292 31, in addition to the tandem array of *gp63* genes on chromosome 10 (47, 65). These
293 related proteases may suppress CXCL10 during different stages of infection or cleave an
294 additional set of host substrates, even though they are not required for CXCL10 cleavage
295 under our *in vitro* conditions. Second, *L. major* Δ *gp63+1* has one of the seven
296 chromosome-10 *gp63* copies maintained on a plasmid under G418 selection and
297 optimized for expression in promastigotes (55), making the currently available GP63

298 strains sub-optimal for *in vivo* experiments. Despite these limitations, we demonstrate that
299 GP63 cleavage of CXCL10 is selective, rapid, and renders the chemokine non-functional.
300 Further investigation beyond the scope of this manuscript will be required to elucidate the
301 implications of CXCL10 cleavage in other infection contexts and animal models.

302 An effective vaccine to protect against leishmaniasis has been a tantalizing
303 strategy for disease control with unrealized potential due to an incomplete understanding
304 of how the parasites interact with the immune system. Historically, inoculation with live
305 parasites in unexposed areas of skin has effectively prevented future infections (66);
306 however, this strategy poses significant risks (67-69) and subsequent vaccine
307 development efforts failed to confer long-term protection in human studies (66). Recent
308 studies highlight the importance of chemokine recruitment in mounting an efficient
309 secondary immune response. Specifically, transcription of *Cxcl10* is upregulated in T
310 resident-memory (T_{rm}) cells after secondary infection, and antibody blockade of CXCR3
311 prevents recruitment of circulating CD4+ T cells to the site of infection (70-72). Together
312 with our finding that CXCR3 substrates are cleaved by *L. major*, this suggests that one of
313 the goals of vaccine development should be to overcome parasite-encoded CXCR3
314 escape upon secondary infection. Promisingly, GP63-specific CD4+ T cells elicit strong
315 IFN γ and T $_h$ 1 responses (73) while GP63 based vaccines elicit long term immunity in mice
316 that is correlated with T $_h$ 1 responses (74-77); a phenotype that could be enhanced by
317 anti-GP63 antibodies functionally blocking cleavage of CXCR3 ligands. A complete
318 understanding of how the parasite alters chemokine recruitment upon secondary infection
319 may facilitate development of a vaccine that can provide long term immunity to
320 leishmaniasis.

321 The relevance of these insights into immune evasion is made more impactful by
322 the observation that CXCL10 suppression has arisen in multiple intracellular pathogens.
323 We found that *L. major*, *S. Typhimurium*, and *C. trachomatis* independently evolved the
324 ability to suppress CXCL10, which indicates that suppression of CXCR3 inflammatory
325 signaling is advantageous for multiple intracellular pathogens. In addition to *S.*
326 *Typhimurium* and *C. trachomatis*, several other commensal and pathogenic bacteria have
327 been reported to suppress CXCL10, including *Lactobacillus paracasei*, *Streptococcus*
328 *pyogenes*, *Fingoldia magna*, and *Porphyromonas gingivalis* (78-80). Similarly, the fungal
329 pathogen *Candida albicans* produces a signaling molecule to inhibit CXCL10 transcription
330 (81). Among viruses, Hepatitis C virus (HCV) upregulates host proteases to modify
331 CXCL10 (82), Epstein-Barr virus (EBV) decreases transcription through chromatin
332 remodeling at the CXCL10 locus (83), and Zika virus (ZIKV) blocks translation of CXCL10
333 (84, 85). The repeated and independent evolution of CXCL10 evasion suggests that this
334 chemokine poses a significant evolutionary pressure on common human pathogens.
335 These diverse pathogens heavily impact global morbidity and mortality. Understanding
336 how pathogens manipulate the CXCR3 signaling axis to their advantage may enable
337 therapeutic countermeasures that circumvent or prevent pathogen suppression of
338 CXCR3 signaling.

339

340 **Materials/Methods**

341 *Cell Lines*

342 LCLs from the International HapMap Project (86) (GM18524 from Han Chinese in Beijing,
343 China, GM19203 from Yoruba in Ibadan, Nigeria, GM7357 from Utah residents with

344 Northern and Western European ancestry from the CEPH collection, and HG02647 of
345 Gambian ancestry isolated in Gambia) were purchased from the Coriell Institute. LCLs
346 were maintained at 37°C in a 5% CO₂ atmosphere and were grown in RPMI 1640 media
347 (Invitrogen) supplemented with 10% fetal bovine serum (FBS), 2 mM glutamine, 100 U/ml
348 penicillin-G, and 100 mg/ml 790 streptomycin. THP-1 monocytes, originally from ATCC,
349 were obtained from the Duke Cell Culture Facility and maintained in RPMI 1640 as
350 described above. HEK293T cells were obtained from ATCC and maintained in DMEM
351 complete media (Invitrogen) supplemented with 10% FBS, 100U/ml penicillin-G, and
352 100mg/ml 790 streptomycin. Jurkat cells (an immortalized T cell line) stably expressing
353 CXCR3 were generated by transfecting a linearized pcDNA3.1 expression vector
354 encoding CXCR3 and resistance to Geneticin (G-418), selecting for transfected cells with
355 1000 µg/mL Geneticin, and collecting highly expressing CXCR3 cells by FACS. Cells
356 were maintained in RPMI 1640 media (Sigma) supplemented with 10% FBS, 1%
357 Penicillin/Streptomycin, 0.23% Glucose, 10mM HEPES, 1mM Sodium Pyruvate, and 250
358 µg/mL Geneticin. The A2EN cell line was provided by Raphael Valdivia and maintained
359 in Keratinocyte serum free media (Gibco; 17005-042) supplemented with 10% heat-
360 inactivated FBS, Epidermal Growth Factor 1-53, and Bovine Pituitary Extract.

361

362 *Pathogen culture and infections.*

363 *Leishmania* spp. were obtained from BEI (*L. major* WT ((MHOM/SN/74/Seidman), NR-
364 48819), *L. major* Δ gp63 ((MHOM/SN/74/SD) Δ gp63 1-7, NR-42489), *L. major* Δ gp63+1
365 (MHOM/SN/74/SD) Δ gp63 1-7 + gp63-1, NR-42490)). Parasites were maintained at 27°C
366 in M199 media (Sigma-Aldrich, M1963), supplemented with 100u/ml

367 penicillin/streptomycin, and 0.05% Hemin (Sigma-Aldrich, 51280). Cultures were split
368 1:20 every 5 days into 10mL of fresh culture media. To prepare parasites for infection,
369 8mL of a 5-day-old culture was spun at 1200g for 10 min and washed with 5mL of HBSS
370 prior to counting promastigotes with a hemocytometer and resuspending at the indicated
371 concentration. As relevant controls in using these *L. major* strains, we found the strains
372 contained similar levels of metacyclic parasites based on flow cytometric measurement
373 (87) and metacyclic enrichment with peanut agglutinin (Fig. S1).

374 For *Leishmania major* infections of LCLs and THP-1 monocytes, 1×10^5 cells were
375 placed in 100 μ l of RPMI 1640 assay media as described above, with no
376 penicillin/streptomycin added. In the case of THP-1 monocytes, cells were then stimulated
377 with 1 μ g/mL of LPS derived from *Salmonella enterica* serovar Typhimurium S-form` (Enzo
378 Bioscience, ALX-581-011-L001). Finally, 1×10^6 *L. major* promastigotes were added in
379 50 μ L of RPMI 1640 assay media for a multiplicity of infection (MOI) of 10. Culture
380 supernatants and cell pellets were collected after 24 hours of infection. For phorbol 12-
381 myristate 13-acetate (PMA) differentiation of THP-1 monocytes, 1.2×10^6 cells were
382 placed in 2mL of complete RPMI 1640 media supplemented with 100ng/mL of PMA for 8
383 hours after which the RPMI media was replaced and cells allowed to rest for 36 hours.
384 Parasites were then washed and counted as described above and added at an MOI of
385 20. At 24 hours post-infection, the culture supernatant was removed, spun at 1200g for
386 10 minutes to separate extracellular parasites, and stored at -20C for downstream
387 cytokine analysis. Cells were then washed 3 times with 1mL of PBS followed by one
388 additional wash with 2mL of RPMI media to remove the remaining extracellular
389 promastigotes. At 48 hours post infection the culture supernatant was collected and

390 stored for downstream analysis. All cells were stored in 1mL of RNAprotect (Qiagen,
391 76526) at -20C for downstream RNA extraction (RNeasy Mini Kit, Qiagen, 74106) and
392 qPCR analysis.

393 Screening GM18524 CXCL10 after infection with *Salmonella enterica* serovar
394 Typhimurium 14028s, *Chlamydia trachomatis* serovar L2, and *Toxoplasma gondii* (RH
395 and Prugniaud A7) were performed as described previously (88). For *Staphylococcus*
396 *aureus*, LCLs were plated at 40,000 cells per 100 μ l RPMI assay media in 96-well plates
397 prior to inoculation at an MOI of 10 with *S. aureus* Sanger-476. Cells were spun at 200xg
398 for 5 minutes prior to incubation at 37°C for 1 hour. Gentamicin was added at 50 μ g/ml
399 and then supernatant was collected at 24 hours. For *Cryptococcus neoformans*, LCLs
400 were plated at 40,000 cells per 100 μ l RPMI assay media in 96-well plates prior to
401 inoculation at an MOI of 5 with *C. neoformans* H99 strain. Cells were incubated at 37°C
402 for 24 hours prior to collection of supernatant. For *Plasmodium berghei* infections, LCLs
403 were plated at 40,000 cells per 100 μ l RPMI assay media in 96-well plates prior to
404 inoculation with 17,000 *P. berghei*-Luciferase sporozoites isolated from *Anopheles*
405 *stephensi* from the New York University Insectary Core Facility. Cells were spun at
406 1000xg for 10 minutes prior to incubation at 37°C for 48 hours. Cell death was monitored
407 by 7AAD staining and quantified using a Guava easyCyte HT flow cytometer. To harvest
408 supernatants, LCLs were centrifuged at 200xg for 5 minutes prior to removing
409 supernatant and storing at -80°C prior to quantifying chemokines production by ELISA.
410 For *Mycobacterium marinum* and *Mycobacterium smegmatis* infections, LCLs were
411 plated at 40,000 cells per 100 μ l RPMI assay media without FBS and supplemented with
412 0.03% bovine serum albumin (BSA) prior to infection with 400,000 bacteria per well. Cells

413 were spun at 100xg for 5 minutes prior to incubation at 33°C for 3 hours, after which 50µl
414 of streptomycin in RPMI media was added for a final concentration of 200µg/ml
415 streptomycin with 10% FBS, and incubation was continued at 33°C for 24 hours. Cell
416 death was monitored by 7AAD staining and quantified using a Guava easyCyte HT flow
417 cytometer. To harvest supernatants, LCLs were centrifuged at 200xg for 5 minutes prior
418 to removing supernatant and storing at -80°C prior to quantifying chemokines by ELISA.

419 Confirmation of suppression by *S. Typhimurium* and *C. trachomatis* in LCL
420 HG02647 was performed in 24 well plate format. For *S. Typhimurium* infection, 5×10^5
421 cells were washed with antibiotic free RPMI assay media and plated in 500µl of RPMI
422 assay media prior to infection at MOI 30. At 1 hour post infection, gentamycin was added
423 at 50µg/mL to kill the remaining extracellular bacteria. At 2 hours post infection,
424 gentamycin was diluted to 18µg/mL to prevent killing of intracellular bacteria. For *C.*
425 *trachomatis* infection, 2×10^5 cells were washed and plated in 500µl of RPMI assay media
426 prior to infection at MOI 5 followed by centrifugation at 1500g for 30 minutes. For *S.*
427 *Typhimurium* infection of THP-1 monocytes, cells were washed once with antibiotic free
428 RPMI assay media and resuspended at a concentration of 1×10^5 in 100µl of RPMI assay
429 media on a 96-well plate. Cells were then treated with 1µg/mL of LPS diluted in RPMI
430 assay media or the equivalent volume of media and *S. typhimurium* added at an MOI of
431 10. At 1 hour post infection, gentamycin was added at 50µg/mL. At 2 hours post infection,
432 gentamycin was diluted to 25 µg/mL. For *C. trachomatis* infection of A2EN cells, 1×10^5
433 cells were plated in a 96 well plate the day prior to infection. *C. trachomatis* was added at
434 an MOI of 5 and centrifuged for 30 minutes at 1500g. For all *S. Typhimurium* infections,
435 culture supernatants were harvested at 24 hours post infection. For *C. trachomatis*

436 infection, culture supernatants were collected cells at 72 hours post infection to assess
437 cytokine production.

438

439 *In vitro T cell migration*

440 RPMI 1640 media (Sigma) was supplemented with 2% FBS and CXCL10 at a starting
441 concentration of 100nM. This was pre-incubated at a ratio of 1:1 with conditioned media
442 from either *L. major* WT, $\Delta gp63$, or $\Delta gp63+1$. After 12 hours of pre-incubation, 600 μ l of
443 CXCL10/conditioned media mix was added to a 24 well plate. 500,000 Jurkat T cells
444 stably transfected with *CXCR3* were seeded onto the apical membrane of the 5 μ m
445 transwell insert (Corning, 3421), and allowed to incubate at 37°C for 4 hours. The
446 transwell insert was removed and the concentration of cells in the basal chamber
447 determined using a Guava easyCyte HT flow cytometer (Millipore).

448

449 *Expression of recombinant GP63 and site directed mutagenesis*

450 Expression of CXCL10 and GP63 were performed by transfection in HEK293T
451 cells. HEK293Ts were maintained in complete DMEM media supplemented with 10%
452 FBS. Two days prior to transfection, 250,000 cells were washed and plated in a 6-well
453 tissue culture treated plate in 2mL of serum free, FreeStyle 293 Expression Media
454 (ThermoFisher, 12338018). One hour prior to transfection, media was replaced with fresh
455 FreeStyle media. Transfection was performed with 2.5 total μ g of endotoxin free plasmid
456 DNA using the Lipofectamine 3000 Transfection Reagent Kit per manufacturer's
457 instructions. Transfected HEK293Ts were incubated at 37°C for 48 hours prior to

458 harvesting culture supernatant and storing in polypropylene, low-binding tubes (Corning,
459 29442-578) at -80°C until use.

460 The CXCL10 plasmid was obtained from Origene (NM_001565), and contains C-
461 terminal Myc and Flag epitope tags. For GP63, a codon optimized plasmid was obtained
462 from OriGene on the pcDNA3.1/Hygro plasmid backbone. Following a kozak sequence
463 and secrecon to enhance secretion (89-91), GP63-1 based on the *L. major* Fd sequence
464 (Q4QHH2-1) was inserted with the *Leishmania* specific secretion signal and GPI anchor
465 motif removed (V100-N577) (92), and epitope tagged with Myc and His sequences placed
466 at the C-terminus. Point mutations in CXCL10 and GP63 were made using the Agilent
467 QuikChange Site Directed Mutagenesis kit according to manufacturer's instructions.

468

469 *Mass spectrometry*

470 CXCL10 exposed to GP63 for 5 hours, along with a negative (untreated) control
471 was delivered in PAGE loading buffer at an approximate concentration of 30 ng/uL. Mass
472 spectrometry was carried out by the Duke Proteomics and Metabolomics Shared
473 Resource. Molecular weight analysis of intact and cleaved CXCL10 from gel loading
474 buffer was performed using a ZipChip CE system (908 Devices, Inc) coupled to a Q
475 Exactive HF Orbitrap mass spectrometer (Thermo Scientific). Ammonium acetate was
476 added to the sample to a final concentration 0.1 M, and 5µL of the loading buffer was
477 pipetted manually into a HR ZipChip. Capillary electrophoresis (CE) separation was
478 performed at 500 V/cm with a 30 second injection in Metabolite BGE (908 Devices, Inc).
479 Mass spectrometry used positive electrospray with 120,000 Rs scan, 500-2000 m/z, 3e6

480 AGC target and 100 msec max ion injection time. Mass deconvolution was performed in
481 Proteome Discoverer 2.2.

482 Tandem mass spectrometric sequencing of the cleaved and uncleaved fragments
483 of CXCL10 after GP63 treatment, as well as an untreated control sample, were performed
484 after gel separation on a 4-12% NuPAGE gel (Invitrogen). Gel bands were isolated after
485 colloidal Coomassie staining, destained in acetonitrile/water, reduced with 10 mM DTT,
486 alkylated with 20 mM iodoacetamide, and digested overnight at 37°C with 300 ng
487 sequencing grade trypsin (Promega) in 50 mM ammonium bicarbonate at pH 8. Peptides
488 were extracted in 1% formic acid and dried on a speedvac, then resuspended in a total
489 of 10 µL 97/2/1 v/v/v water/acetonitrile/TFA. 4 µL of each sample was injected for analysis
490 by LC-MS/MS using a 90 minute, 5-30% MeCN LC gradient and a top 12 DDA MS/MS
491 method with MS1 at 120k and MS2 at 15k resolution. The data files were searched on
492 Mascot v 2.5 with the UniProt database (downloaded November 2017) and *Homo sapiens*
493 taxonomy selected, semitryptic specificity, along with fixed modification carbamidomethyl
494 (C) and variable modifications oxidated (M), and deamidated (NQ). The results of the
495 database searches were compiled into Scaffold v4 for curation. Using the search results
496 as a spectral library, Skyline v4.1 was used to extract peak intensities for peptides which
497 looked to be a part of the cleavage region (residues 74-91) or non-cleaved region
498 (residues 48-68), in order to more definitively localize the specific cleavage location
499 (Figure 2E). Intensity was expressed as the peak area normalized to the protein region
500 from residues 29-52, in order to control for protein abundance differences between the
501 samples. The Skyline file has been made publicly available at Panoramaweb.org
502 (<https://goo.gl/4xsLsF>).

503

504 *Statistical analysis*

505 All statistical analysis was performed using GraphPad Prism. Unpaired Student's *t*-test,
506 one-way ANOVA, and two-way ANOVA with Tukey's post-hoc test were used as
507 appropriate where indicated. The number of biological replicates (N) are indicated in the
508 figure legend for each experiment and defined as follows. For *in vitro* cell culture and
509 protein assessment each well of cells or chemokine prior to experimental manipulation
510 (such as infection with parasite or addition of chemokine and/or inhibitor) was treated as
511 a unique biological replicate. When technical replicates, repeated use of the same
512 biological sample in a readout assay, were used they are indicated in the figure legend
513 text and averaged values were combined into the single biological replicate prior to
514 calculating statistics.

515

516 **Acknowledgments**

517 ALA, KDG, ET, KJP, BHS, and DCK were supported by Duke Molecular Genetics &
518 Microbiology startup funds, Duke University Whitehead Scholarship, Butler Pioneer
519 Award, and NIH U19AI084044. ET was supported by the Duke Summer Research
520 Opportunity Program (SROP). JSS and SR were supported by NIH GM122798 and the
521 Burroughs Wellcome Fund Career Award for Medical Scientists. RLR was supported by
522 NIH AI119004. We thank Robyn Guo for assistance with immunoblotting, Sarah Rains for
523 assistance with sample prep for CXCL10 cleavage site identification, and Jeffrey S.
524 Bourgeois for thoughtful discussion about experimental design and analysis. We thank
525 the Duke University School of Medicine for the use of the Proteomics and Metabolomics
526 Shared Resource.

527

528 **Author contributions**

529 All authors critically reviewed the manuscript and contributed input to the final submission.

530 ALA, DCK, KDG, and RLR wrote the manuscript. ALA, DCK, RLR, JSS, SR, and JWT

531 contributed to strategy and project planning. ALA, KDG, ET, KJP, BHS, JSS, JWT, RLR,

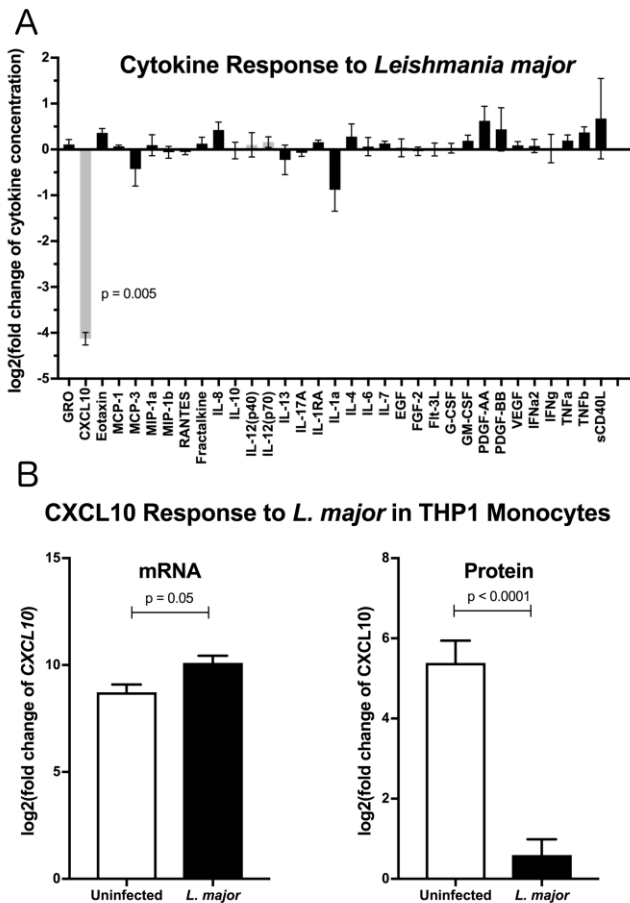
532 and DCK carried out experiments and analysis.

533

534 **Competing Interests**

535 The authors declare that no competing interests exist.

536



537

538 **Figure 1. *Leishmania major* suppresses CXCL10 post-transcriptionally in multiple**

539 **human cell lines (A) Cytokine screening of LCLs exposed to *L. major* demonstrated**

540 **suppression of CXCL10. Three lymphoblastoid cell lines (LCL), 7357, 18524, and 19203,**

541 **were infected with *L. major*. Chemokines secreted into culture supernatants were**

542 **analyzed by Luminex. Cytokines below the limit of detection were removed from the final**

543 **analysis. Values are represented as log₂ of the fold change relative to uninfected LCLs.**

544 **Type-1 associated cytokines are represented in grey. P value represents Dunnett's post-**

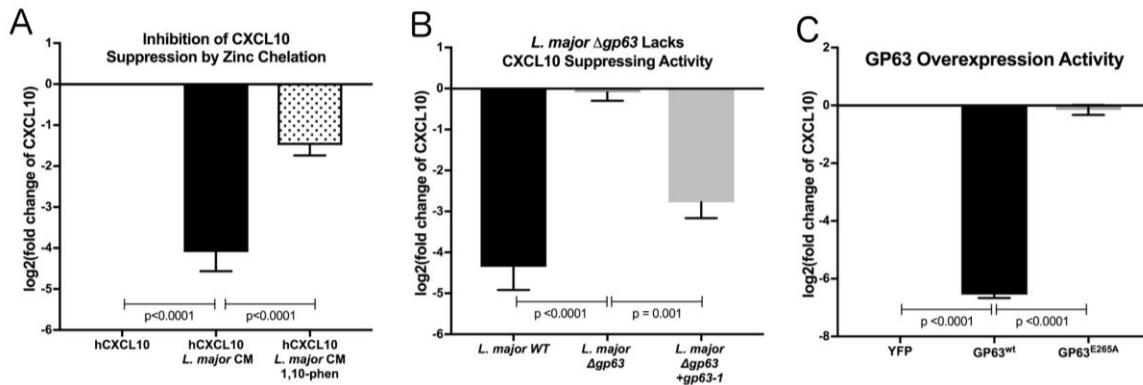
545 **hoc test compared to 1, after repeated measures one-way ANOVA. (B) CXCL10**

546 **produced by LPS stimulated THP-1 monocytes was suppressed by *L. major*. THP-1**

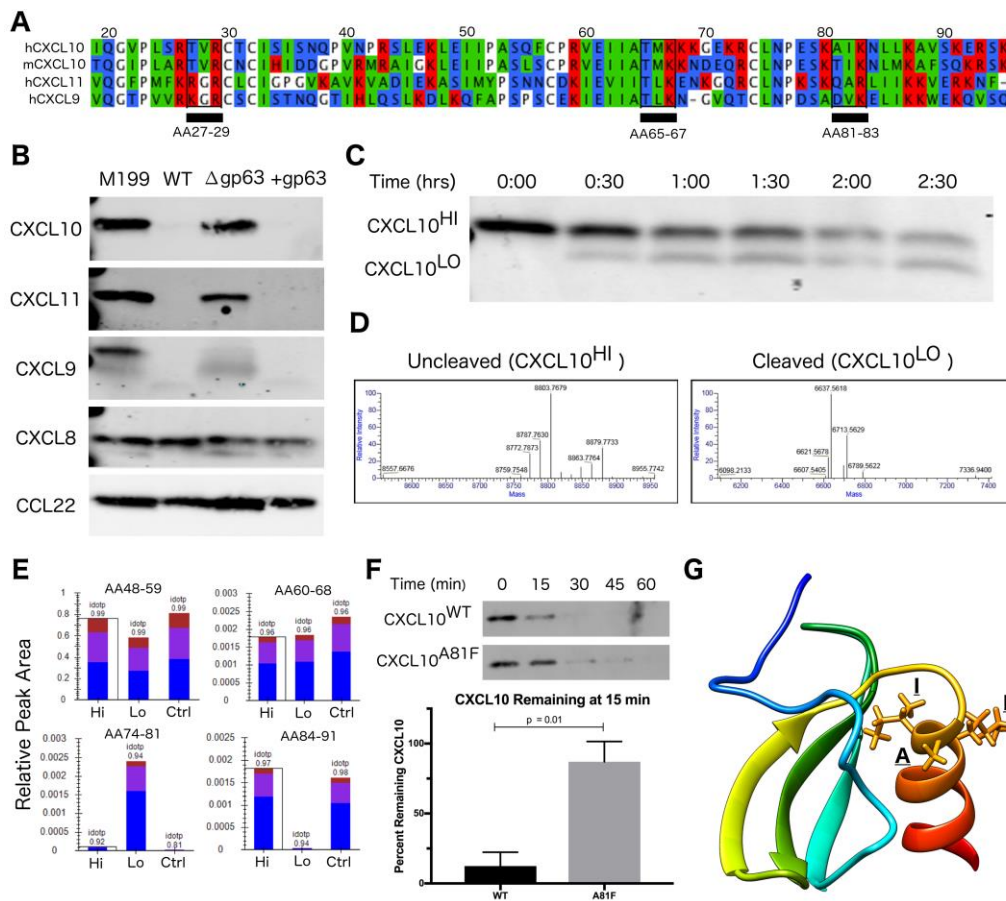
547 **monocytes were stimulated with LPS prior to *L. major* infection. CXCL10 mRNA was**

548 **measured by qRT-PCR TaqMan assay using the $\Delta\Delta C_t$ method with 18s as housekeeping**

549 gene, and CXCL10 protein was measured by ELISA. For mRNA (n=3) and ELISA (n=6),
550 Fold Change is relative to unstimulated, uninfected THP-1s. P values calculated by
551 Student's *t*-test.



552
553 **Figure 2. *Leishmania major* matrix-metalloprotease, glycoprotein-63, is necessary**
554 **and sufficient to cleave CXCL10.** (A) Zinc chelation prevents CXCL10 suppression.
555 Concentration of human recombinant CXCL10 was measured by ELISA after incubation
556 for 12 hours with filtered conditioned media from *L. major* WT promastigote culture and
557 addition of the zinc-chelator 1,10-phenanthroline (n=8). (B) *gp63* is required for *L. major*
558 CXCL10 suppression. Human recombinant CXCL10 concentrations were measured by
559 ELISA after 12 hour incubation with conditioned media from *L. major* WT, $\Delta gp63$, or
560 $\Delta gp63+1$ (n=6). (C) GP63 expressed and secreted by HEK293Ts is sufficient for CXCL10
561 suppression. Human recombinant CXCL10 concentrations were measured by ELISA
562 after 12 hour incubation with culture supernatant from HEK293Ts transfected with
563 pCDNA3.1-*gp63*^{WT} or pCDNA3.1-*gp63*^{E285A} (n=7). P values calculated by one-way
564 ANOVA with Tukey's post-hoc test. Error bars represent standard error of the mean.

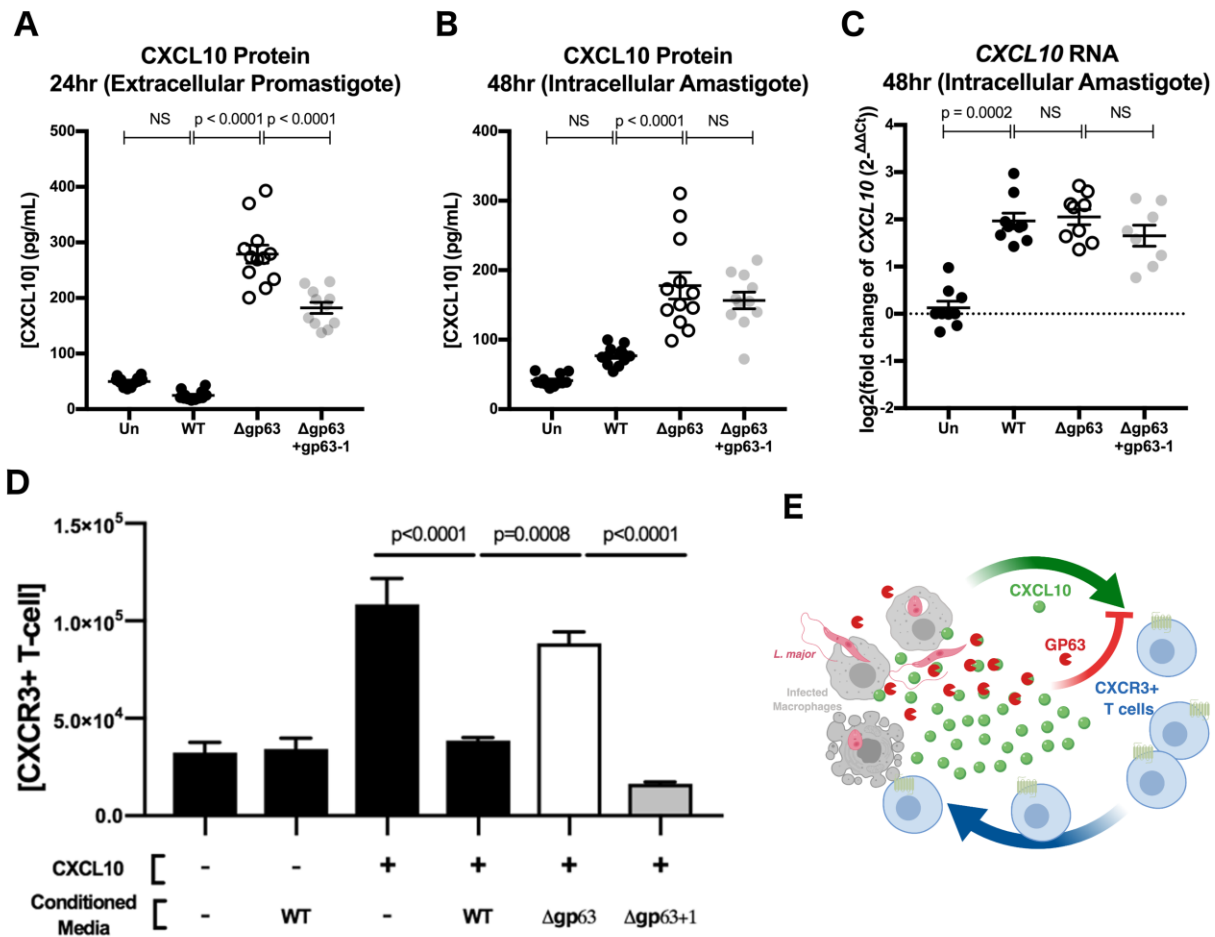


565

566 **Figure 3. CXCL10 cleavage by GP63 occurs between positions A81 and I82.** (A)
 567 CXCL9/10/11 share significant homology at the amino-acid level. Multisequence alignment
 568 demonstrates that physical characteristics of amino acids are conserved across the CXCL10
 569 family of chemokines. There are three putative GP63 cleavage sites (underlined) based on the
 570 consensus sequence of polar (P1), hydrophobic (P1'), basic (P2') (53). (B) GP63 selectively
 571 cleaves chemokine ligands of the CXCR3 receptor. Conditioned media from *L. major* WT, $\Delta gp63$,
 572 and $\Delta gp63+1$ was incubated with human recombinant chemokines for 12 hours and product
 573 detected by western blot. Cleavage is only detected for the CXCL9/10/11 family. (C) Cleavage by
 574 GP63 generates a smaller molecular weight protein. A time course of cleavage of human CXCL10
 575 by heterologously expressed GP63 demonstrated an intermediate cleavage product, resolved by
 576 PAGE and Coomassie staining. (D) Cleavage by GP63 results in a change in CXCL10 molecular

577 weight of 2.2kD. Capillary electrophoresis-Mass Spectrometry (CE-MS) determined the molecular
578 weight of the uncleaved (CXCL10^{Hi}) and cleaved (CXCL10^{Lo}) bands as 8.8kD and 6.6kD
579 respectively. (E) Comparative analysis by trypsin digest of cleaved and uncleaved CXCL10
580 reveals cleavage occurring between A81-I82. Liquid chromatography-mass spectrometry (LC-
581 MS) following trypsin digest of CXCL10^{Hi} and CXCL10^{Lo} identified peptide ending at A81,
582 exclusively in the CXCL10^{Lo} band, and a corresponding lack of peptide coverage from AA84-91.
583 (F) Mutation of A81F significantly impairs GP63 cleavage of CXCL10. In the presence of GP63,
584 CXCL10^{A81F} remains stable for up to 45 minutes whereas CXCL10^{WT} degradation is nearly
585 complete by 15 minutes. Percentage of GP63 remaining at 15 minutes is plotted (n=3-4 per
586 CXCL10 genotype). P value calculated by Student's *t-test*. (G) The GP63 cleavage site is found
587 on the C-terminal alpha-helix loop of CXCL10. Based on the NMR crystal structure of CXCL10
588 (Booth et al., 2002), the A81, I82, K83 (P1, P1', P2') GP63 cleavage motif maps to an exposed
589 alpha-helical region.

590



591

592

593 **Figure 4. GP63 produced by *L. major* promastigotes and amastigotes cleaves**

594 **CXCL10 and abolishes its chemotactic activity.** (A) *L. major* promastigotes suppress

595 CXCL10 through GP63 activity. THP-1 monocytes were differentiated using 100ng/mL of

596 PMA prior to infection and CXCL10 concentration was assessed in the supernatant 24

597 hours post-infection by ELISA. (B) *L. major* amastigotes suppress CXCL10 through GP63

598 activity. At 24 hours post-infection, extracellular promastigotes were washed away from

599 the differentiated THP-1 monocytes. At 48 hours post-infection the CXCL10 concentration

600 was assessed in the supernatant by ELISA. For A-B, data represents four separate
601 infections and was analyzed by one-way ANOVA with Tukey's post-hoc test (C) *L. major*
602 induces similar levels of *CXCL10* mRNA, independent of GP63 genotype. At 48 hours
603 post-infection, mRNA was extracted from PMA differentiated THP-1 monocytes and
604 *CXCL10* mRNA was measured by qRT-PCR TaqMan assay using the $\Delta\Delta C_t$ method with
605 18s as housekeeping gene. For C, data are from three separate experiments and were
606 analyzed by one-way ANOVA with Tukey's post-hoc test. (D) *CXCL10* incubated with
607 GP63 is unable to chemoattract CXCR3+ cells *in vitro*. Jurkat T cells stably transfected
608 with CXCR3 were seeded on the apical surface of a 5 μ m transwell insert, with human
609 recombinant *CXCL10* pre-incubated with conditioned media from either *L. major* WT,
610 $\Delta gp63$, or $\Delta gp63+1$ in the basal chamber. The number of CXCR3+ Jurkats in the basal
611 chamber after 4 hours were counted to assess chemotactic capacity of *CXCL10* after
612 exposure to GP63. (E) Proposed model where the host attempts to upregulate *CXCL10*
613 in response to infection, but through the activity of GP63 *L. major* is able to impair
614 signaling through the CXCR3 receptor.

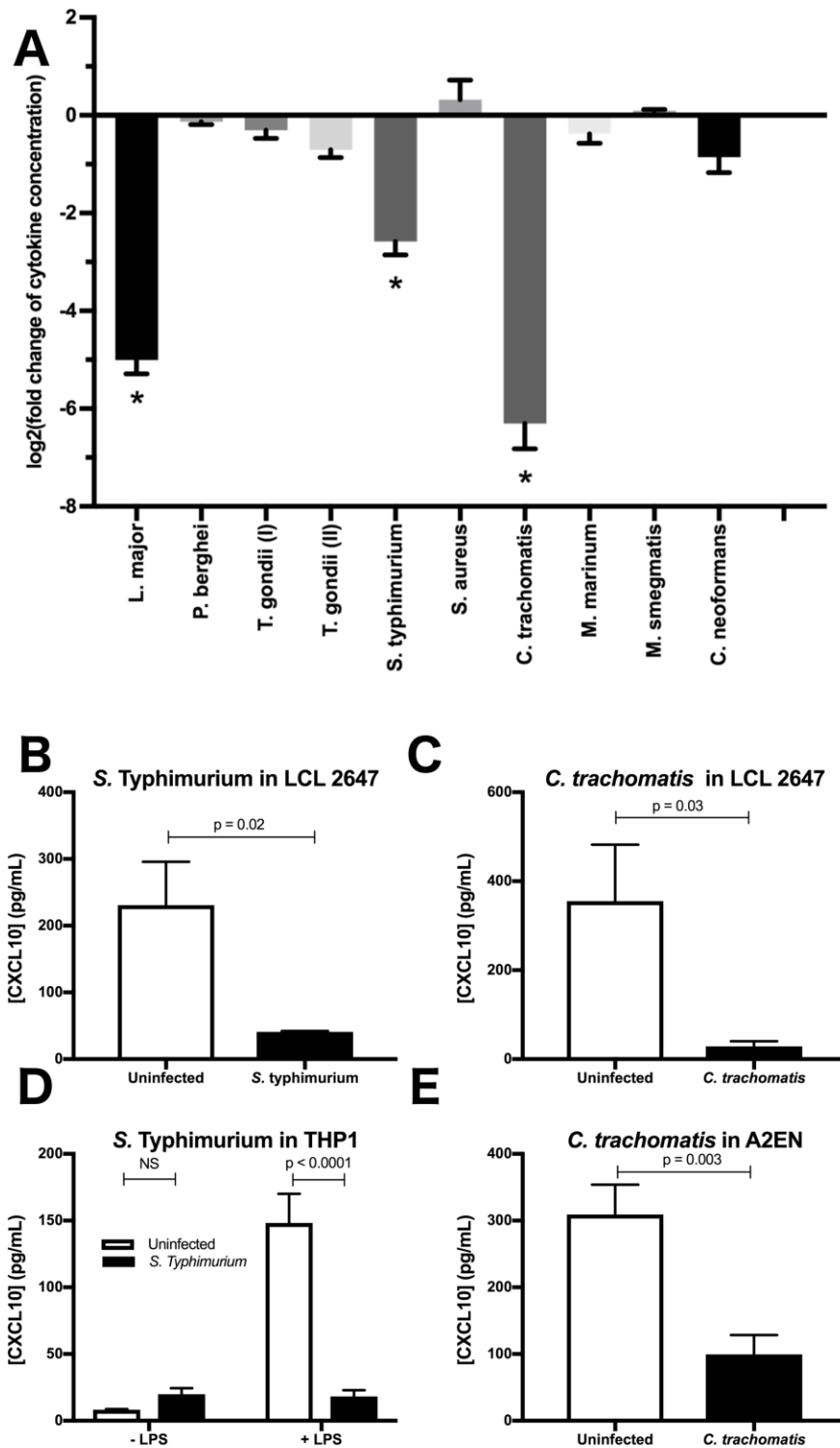
615

616

617

618

619



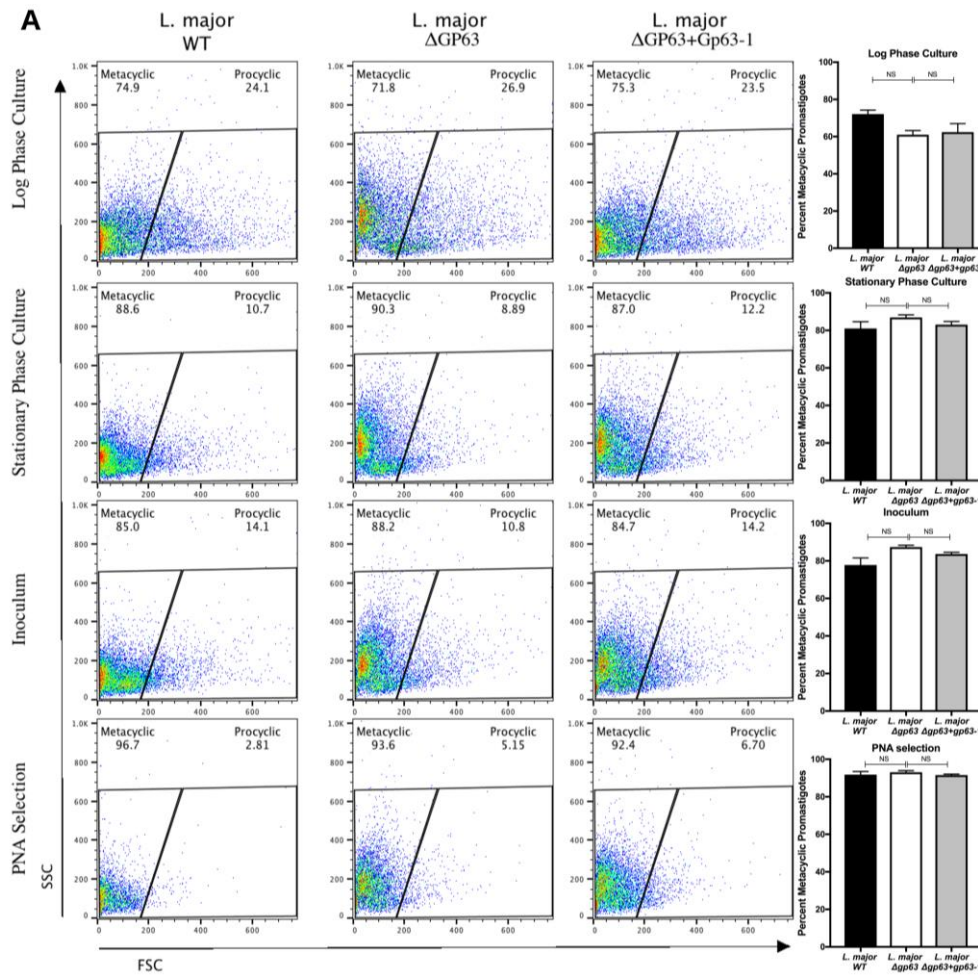
620

621 **Figure 5. Multiple intracellular pathogens have evolved a mechanism for CXCL10**

622 **suppression.** (A) LCL 18524 was used to screen *L. major* (*p*=0.0001), *P. berghei*

623 (p=0.99), *T. gondii* I (RH) (p=0.44), *T. gondii* II (Prugniaud A7) (p=0.011), *S. enterica*
624 serovar Typhimurium (p=0.0001), *S. aureus* (p=0.12), *C. trachomatis* (p=0.0001), *M.*
625 *marinum* (p=0.37), *M. smegmatis* (p>0.99), and *C. neoformans* (p=0.010) for CXCL10
626 suppressing activity (n=2-4 for each pathogen). CXCL10 concentration was measured by
627 ELISA and is represented as the log₂ of fold change relative to uninfected controls. P
628 values calculated by one-way ANOVA with Dunnett's post-hoc test comparing non-log
629 transformed values to 1, which would represent no change relative to uninfected. (*)
630 represents p<0.01. (B-C) *S. Typhimurium* and *C. trachomatis* suppress CXCL10 in a
631 second LCL. Infections were performed in the LCL HG02647 for *S. Typhimurium* (n=6;
632 two experiments) and *C. trachomatis* (n=5; three experiments). Mean +/- standard error
633 of the mean is plotted and P values calculated by Student's *t-test*. (D) *S. Typhimurium*
634 suppresses production of CXCL10 in THP-1 monocytes. THP-1 monocytes were
635 stimulated with 1µg/mL of purified LPS from *S. Typhimurium* at the time of infection.
636 CXCL10 concentration in culture supernatant at 24hpi was assayed by ELISA. Mean +/-
637 standard error the mean is plotted, and P values calculated by two-way ANOVA with
638 Tukey's post-hoc test. (E) *C. trachomatis* suppresses CXCL10 in the human endocervical
639 epithelial cell line A2EN. CXCL10 concentration in culture supernatant at 72hpi was
640 assayed by ELISA. Mean +/- standard error of the mean is plotted and P values calculated
641 by Student's *t-test*.

642



643

644 **Figure S1.** *L. major* WT, *L. major* Δ gp63, and *L. major* Δ gp63+1 undergo comparable
645 rates of metacyclogenesis. (A) Flow cytometry and selection with peanut agglutinin (PNA)
646 demonstrate that the three strains of *L. major* used in this study did not have significantly
647 different rates of metacyclogenesis. Parasites were analyzed using a Guava EasyCyte-
648 HT flow cytometer and gated based on forward scatter (FSC) and side scatter (SSC) as
649 previously described (87). Log-phase parasites were obtained from day 3 of culture,
650 stationary phase parasites from day 5 of culture, the inoculum from day 5 culture after
651 preparing parasites for infection as described in methods, and PNA selected from the
652 inoculum after PNA selection. PNA selection was performed by incubating 1×10^8
653 parasites in 100 μ g/mL of PNA (Vector Labs, L-1070-5) for 30 minutes at room

654 temperature, followed by spinning for 5 minutes at 200xg, and taking the PNA- parasites
655 in the supernatant for analysis. The PNA- parasites were then used as a control to define
656 the gate for metacyclic promastigotes based on FSC and SSC. Conditions (n = 3 per
657 group) were analyzed by one-way ANOVA with Tukeys post-hoc test. Not significant (NS)
658 indicated $p > 0.05$.
659

- 660 1. **Reiner SL, Locksley RM.** 1995. The regulation of immunity to *Leishmania major*.
661 *Annu Rev Immunol* **13**:151-177.
- 662 2. **Alvar J, Velez ID, Bern C, Herrero M, Desjeux P, Cano J, Jannin J, den Boer M,**
663 **Team WHOLC.** 2012. Leishmaniasis worldwide and global estimates of its
664 incidence. *PLoS One* **7**:e35671.
- 665 3. **Okwor I, Uzonna JE.** 2009. Immunotherapy as a strategy for treatment of
666 leishmaniasis: a review of the literature. *Immunotherapy* **1**:765-776.
- 667 4. **Hajishengallis G, Lambris JD.** 2011. Microbial manipulation of receptor crosstalk
668 in innate immunity. *Nat Rev Immunol* **11**:187-200.
- 669 5. **Finlay BB, McFadden G.** 2006. Anti-immunology: evasion of the host immune
670 system by bacterial and viral pathogens. *Cell* **124**:767-782.
- 671 6. **Scott P, Novais FO.** 2016. Cutaneous leishmaniasis: immune responses in
672 protection and pathogenesis. *Nat Rev Immunol* **16**:581-592.
- 673 7. **Kim CH, Rott L, Kunkel EJ, Genovese MC, Andrew DP, Wu L, Butcher EC.** 2001.
674 Rules of chemokine receptor association with T cell polarization in vivo. *J Clin Invest*
675 **108**:1331-1339.
- 676 8. **Reiner SL, Locksley RM.** 1993. Cytokines in the differentiation of Th1/Th2 CD4+
677 subsets in leishmaniasis. *J Cell Biochem* **53**:323-328.
- 678 9. **Heinzel FP, Sadick MD, Holaday BJ, Coffman RL, Locksley RM.** 1989. Reciprocal
679 expression of interferon gamma or interleukin 4 during the resolution or
680 progression of murine leishmaniasis. Evidence for expansion of distinct helper T cell
681 subsets. *J Exp Med* **169**:59-72.
- 682 10. **Scott P, Natovitz P, Coffman RL, Pearce E, Sher A.** 1988. CD4+ T cell subsets in
683 experimental cutaneous leishmaniasis. *Mem Inst Oswaldo Cruz* **83 Suppl 1**:256-
684 259.
- 685 11. **Uzonna JE, Joyce KL, Scott P.** 2004. Low dose *Leishmania major* promotes a
686 transient T helper cell type 2 response that is down-regulated by interferon gamma-
687 producing CD8+ T cells. *J Exp Med* **199**:1559-1566.
- 688 12. **Belkaid Y, Von Stebut E, Mendez S, Lira R, Caler E, Bertholet S, Udey MC, Sacks**
689 **D.** 2002. CD8+ T cells are required for primary immunity in C57BL/6 mice following
690 low-dose, intradermal challenge with *Leishmania major*. *J Immunol* **168**:3992-4000.
- 691 13. **Muller I, Kropf P, Louis JA, Milon G.** 1994. Expansion of gamma interferon-
692 producing CD8+ T cells following secondary infection of mice immune to
693 *Leishmania major*. *Infect Immun* **62**:2575-2581.
- 694 14. **Muller I, Kropf P, Etges RJ, Louis JA.** 1993. Gamma interferon response in
695 secondary *Leishmania major* infection: role of CD8+ T cells. *Infect Immun* **61**:3730-
696 3738.
- 697 15. **Ritter U, Korner H.** 2002. Divergent expression of inflammatory dermal
698 chemokines in cutaneous leishmaniasis. *Parasite Immunol* **24**:295-301.
- 699 16. **Ajdary S, Alimohammadian MH, Eslami MB, Kemp K, Kharazmi A.** 2000.
700 Comparison of the immune profile of nonhealing cutaneous Leishmaniasis patients
701 with those with active lesions and those who have recovered from infection. *Infect*
702 *Immun* **68**:1760-1764.
- 703 17. **Carvalho EM, Correia Filho D, Bacellar O, Almeida RP, Lessa H, Rocha H.** 1995.
704 Characterization of the immune response in subjects with self-healing cutaneous
705 leishmaniasis. *Am J Trop Med Hyg* **53**:273-277.

- 706 18. **Castellano LR, Filho DC, Argiro L, Dessen H, Prata A, Dessen A, Rodrigues V.**
707 2009. Th1/Th2 immune responses are associated with active cutaneous
708 leishmaniasis and clinical cure is associated with strong interferon-gamma
709 production. *Hum Immunol* **70**:383-390.
- 710 19. **Groom JR, Luster AD.** 2011. CXCR3 ligands: redundant, collaborative and
711 antagonistic functions. *Immunol Cell Biol* **89**:207-215.
- 712 20. **Vargas-Inchaustegui DA, Hogg AE, Tulliano G, Llanos-Cuentas A, Arevalo J,**
713 **Endsley JJ, Soong L.** 2010. CXCL10 production by human monocytes in response to
714 *Leishmania braziliensis* infection. *Infect Immun* **78**:301-308.
- 715 21. **Antoniazzi S, Price HP, Kropf P, Freudenberg MA, Galanos C, Smith DF, Muller I.**
716 2004. Chemokine gene expression in toll-like receptor-competent and -deficient
717 mice infected with *Leishmania major*. *Infect Immun* **72**:5168-5174.
- 718 22. **Zaph C, Scott P.** 2003. Interleukin-12 regulates chemokine gene expression during
719 the early immune response to *Leishmania major*. *Infect Immun* **71**:1587-1589.
- 720 23. **Oghumu S, Dong R, Varikuti S, Shawler T, Kampfrath T, Terrazas CA, Lezama-**
721 **Davila C, Ahmer BM, Whitacre CC, Rajagopalan S, Locksley R, Sharpe AH,**
722 **Satoskar AR.** 2013. Distinct populations of innate CD8+ T cells revealed in a CXCR3
723 reporter mouse. *J Immunol* **190**:2229-2240.
- 724 24. **Barbi J, Oghumu S, Rosas LE, Carlson T, Lu B, Gerard C, Lezama-Davila CM,**
725 **Satoskar AR.** 2007. Lack of CXCR3 delays the development of hepatic inflammation
726 but does not impair resistance to *Leishmania donovani*. *J Infect Dis* **195**:1713-1717.
- 727 25. **Barbi J, Brombacher F, Satoskar AR.** 2008. T cells from *Leishmania major*-
728 susceptible BALB/c mice have a defect in efficiently up-regulating CXCR3 upon
729 activation. *J Immunol* **181**:4613-4620.
- 730 26. **Vasquez RE, Soong L.** 2006. CXCL10/gamma interferon-inducible protein 10-
731 mediated protection against *Leishmania amazonensis* infection in mice. *Infect*
732 *Immun* **74**:6769-6777.
- 733 27. **Gupta G, Bhattacharjee S, Bhattacharyya S, Bhattacharya P, Adhikari A,**
734 **Mukherjee A, Bhattacharyya Majumdar S, Majumdar S.** 2009. CXC chemokine-
735 mediated protection against visceral leishmaniasis: involvement of the
736 proinflammatory response. *J Infect Dis* **200**:1300-1310.
- 737 28. **Gupta G, Majumdar S, Adhikari A, Bhattacharya P, Mukherjee AK, Majumdar**
738 **SB, Majumdar S.** 2011. Treatment with IP-10 induces host-protective immune
739 response by regulating the T regulatory cell functioning in *Leishmania donovani*-
740 infected mice. *Med Microbiol Immunol* **200**:241-253.
- 741 29. **Vester B, Muller K, Solbach W, Laskay T.** 1999. Early gene expression of NK cell-
742 activating chemokines in mice resistant to *Leishmania major*. *Infect Immun*
743 **67**:3155-3159.
- 744 30. **Gondek DC, Roan NR, Starnbach MN.** 2009. T cell responses in the absence of IFN-
745 gamma exacerbate uterine infection with *Chlamydia trachomatis*. *J Immunol*
746 **183**:1313-1319.
- 747 31. **Morrison RP, Caldwell HD.** 2002. Immunity to murine chlamydial genital infection.
748 *Infect Immun* **70**:2741-2751.
- 749 32. **Morrison SG, Farris CM, Sturdevant GL, Whitmire WM, Morrison RP.** 2011.
750 Murine *Chlamydia trachomatis* genital infection is unaltered by depletion of CD4+ T
751 cells and diminished adaptive immunity. *J Infect Dis* **203**:1120-1128.

- 752 33. **Perry LL, Feilzer K, Caldwell HD.** 1997. Immunity to Chlamydia trachomatis is
753 mediated by T helper 1 cells through IFN-gamma-dependent and -independent
754 pathways. *J Immunol* **158**:3344-3352.
- 755 34. **Rank RG, Lacy HM, Goodwin A, Sikes J, Whittimore J, Wyrick PB, Nagarajan UM.**
756 2010. Host chemokine and cytokine response in the endocervix within the first
757 developmental cycle of Chlamydia muridarum. *Infect Immun* **78**:536-544.
- 758 35. **Lijek RS, Helble JD, Olive AJ, Seiger KW, Starnbach MN.** 2018. Pathology after
759 Chlamydia trachomatis infection is driven by nonprotective immune cells that are
760 distinct from protective populations. *Proc Natl Acad Sci U S A* **115**:2216-2221.
- 761 36. **Maxion HK, Kelly KA.** 2002. Chemokine expression patterns differ within
762 anatomically distinct regions of the genital tract during Chlamydia trachomatis
763 infection. *Infect Immun* **70**:1538-1546.
- 764 37. **Hess J, Ladel C, Miko D, Kaufmann SH.** 1996. Salmonella typhimurium aroA-
765 infection in gene-targeted immunodeficient mice: major role of CD4+ TCR-alpha
766 beta cells and IFN-gamma in bacterial clearance independent of intracellular
767 location. *J Immunol* **156**:3321-3326.
- 768 38. **Ravindran R, Foley J, Stoklasek T, Glimcher LH, McSorley SJ.** 2005. Expression of
769 T-bet by CD4 T cells is essential for resistance to Salmonella infection. *J Immunol*
770 **175**:4603-4610.
- 771 39. **Gilchrist JJ, MacLennan CA, Hill AV.** 2015. Genetic susceptibility to invasive
772 Salmonella disease. *Nat Rev Immunol* **15**:452-463.
- 773 40. **Saliba AE, Li L, Westermann AJ, Appenzeller S, Stapels DA, Schulte LN, Helaine
774 S, Vogel J.** 2016. Single-cell RNA-seq ties macrophage polarization to growth rate of
775 intracellular Salmonella. *Nat Microbiol* **2**:16206.
- 776 41. Jul 2015. 7. Replication of Salmonella enterica Serovar Typhimurium in Human
777 Monocyte-Derived Macrophages. *Infect Immun*, 83.2661-2671.
778 <http://iai.asm.org/lookup/doi/10.1128/IAI.00033-15>.
- 779 42. **Martinez FO, Gordon S, Locati M, Mantovani A.** 2006. Transcriptional profiling of
780 the human monocyte-to-macrophage differentiation and polarization: new
781 molecules and patterns of gene expression. *J Immunol* **177**:7303-7311.
- 782 43. **Goldberg MF, Roeske EK, Ward LN, Pengo T, Dileepan T, Kotov DI, Jenkins MK.**
783 2018. Salmonella Persist in Activated Macrophages in T Cell-Sparse Granulomas but
784 Are Contained by Surrounding CXCR3 Ligand-Positioned Th1 Cells. *Immunity*
785 **49**:1090-1102 e1097.
- 786 44. **Chami B, Yeung A, Buckland M, Liu H, G MF, Tao K, Bao S.** 2017. CXCR3 plays a
787 critical role for host protection against Salmonellosis. *Sci Rep* **7**:10181.
- 788 45. **Khan IA, MacLean JA, Lee FS, Casciotti L, DeHaan E, Schwartzman JD, Luster AD.**
789 2000. IP-10 is critical for effector T cell trafficking and host survival in Toxoplasma
790 gondii infection. *Immunity* **12**:483-494.
- 791 46. **Olive AJ, Gondek DC, Starnbach MN.** 2011. CXCR3 and CCR5 are both required for
792 T cell-mediated protection against C. trachomatis infection in the murine genital
793 mucosa. *Mucosal Immunol* **4**:208-216.
- 794 47. **Valdivia HO, Scholte LL, Oliveira G, Gabaldon T, Bartholomeu DC.** 2015. The
795 Leishmania metaphylome: a comprehensive survey of Leishmania protein
796 phylogenetic relationships. *BMC Genomics* **16**:887.

- 797 48. **Olivier M, Atayde VD, Isnard A, Hassani K, Shio MT.** 2012. Leishmania virulence
798 factors: focus on the metalloprotease GP63. *Microbes Infect* **14**:1377-1389.
- 799 49. **Voth BR, Kelly BL, Joshi PB, Ivens AC, McMaster WR.** 1998. Differentially
800 expressed Leishmania major gp63 genes encode cell surface leishmanolysin with
801 distinct signals for glycosylphosphatidylinositol attachment. *Mol Biochem Parasitol*
802 **93**:31-41.
- 803 50. **Fernandes MC, Dillon LA, Belew AT, Bravo HC, Mosser DM, El-Sayed NM.** 2016.
804 Dual Transcriptome Profiling of Leishmania-Infected Human Macrophages Reveals
805 Distinct Reprogramming Signatures. *MBio* **7**.
- 806 51. **Chaudhuri G, Chaudhuri M, Pan A, Chang KP.** 1989. Surface acid proteinase
807 (gp63) of Leishmania mexicana. A metalloenzyme capable of protecting liposome-
808 encapsulated proteins from phagolysosomal degradation by macrophages. *J Biol*
809 *Chem* **264**:7483-7489.
- 810 52. **Joshi PB, Kelly BL, Kamhawi S, Sacks DL, McMaster WR.** 2002. Targeted gene
811 deletion in Leishmania major identifies leishmanolysin (GP63) as a virulence factor.
812 *Mol Biochem Parasitol* **120**:33-40.
- 813 53. **Bouvier J, Schneider P, Etges R, Bordier C.** 1990. Peptide substrate specificity of
814 the membrane-bound metalloprotease of Leishmania. *Biochemistry* **29**:10113-
815 10119.
- 816 54. **Booth V, Keizer DW, Kamphuis MB, Clark-Lewis I, Sykes BD.** 2002. The CXCR3
817 binding chemokine IP-10/CXCL10: structure and receptor interactions.
818 *Biochemistry* **41**:10418-10425.
- 819 55. **Joshi PB, Sacks DL, Modi G, McMaster WR.** 1998. Targeted gene deletion of
820 Leishmania major genes encoding developmental stage-specific leishmanolysin
821 (GP63). *Mol Microbiol* **27**:519-530.
- 822 56. **Muller K, van Zandbergen G, Hansen B, Laufs H, Jahnke N, Solbach W, Laskay T.**
823 2001. Chemokines, natural killer cells and granulocytes in the early course of
824 Leishmania major infection in mice. *Med Microbiol Immunol* **190**:73-76.
- 825 57. **Majumder S, Bhattacharjee S, Paul Chowdhury B, Majumdar S.** 2012. CXCL10 is
826 critical for the generation of protective CD8 T cell response induced by antigen
827 pulsed CpG-ODN activated dendritic cells. *PLoS One* **7**:e48727.
- 828 58. **Vasquez RE, Xin L, Soong L.** 2008. Effects of CXCL10 on dendritic cell and CD4+ T-
829 cell functions during Leishmania amazonensis infection. *Infect Immun* **76**:161-169.
- 830 59. **Qin S, Rottman JB, Myers P, Kassam N, Weinblatt M, Loetscher M, Koch AE,**
831 **Moser B, Mackay CR.** 1998. The chemokine receptors CXCR3 and CCR5 mark
832 subsets of T cells associated with certain inflammatory reactions. *J Clin Invest*
833 **101**:746-754.
- 834 60. **Thomas SY, Hou R, Boyson JE, Means TK, Hess C, Olson DP, Strominger JL,**
835 **Brenner MB, Gumperz JE, Wilson SB, Luster AD.** 2003. CD1d-restricted NKT cells
836 express a chemokine receptor profile indicative of Th1-type inflammatory homing
837 cells. *J Immunol* **171**:2571-2580.
- 838 61. **Cella M, Jarrossay D, Facchetti F, Alebardi O, Nakajima H, Lanzavecchia A,**
839 **Colonna M.** 1999. Plasmacytoid monocytes migrate to inflamed lymph nodes and
840 produce large amounts of type I interferon. *Nat Med* **5**:919-923.
- 841 62. **Nanki T, Takada K, Komano Y, Morio T, Kanegane H, Nakajima A, Lipsky PE,**
842 **Miyasaka N.** 2009. Chemokine receptor expression and functional effects of

- 843 chemokines on B cells: implication in the pathogenesis of rheumatoid arthritis.
844 *Arthritis Res Ther* **11**:R149.
- 845 63. **Hu JK, Kagari T, Clingan JM, Matloubian M.** 2011. Expression of chemokine
846 receptor CXCR3 on T cells affects the balance between effector and memory CD8 T-
847 cell generation. *Proc Natl Acad Sci U S A* **108**:E118-127.
- 848 64. **Harris TH, Banigan EJ, Christian DA, Konradt C, Wojno EDT, Norose K, Wilson**
849 **EH, John B, Weninger W, Luster AD, Liu AJ, Hunter CA.** 2012. Generalized Levy
850 walks and the role of chemokines in migration of effector CD8(+) T cells. *Nature*
851 **486**:545-U145.
- 852 65. **Ivens AC, Peacock CS, Worthey EA, Murphy L, Aggarwal G, Berriman M, Sisk E,**
853 **Rajandream MA, Adlem E, Aert R, Anupama A, Apostolou Z, Attipoe P, Bason N,**
854 **Bauser C, Beck A, Beverley SM, Bianchetti G, Borzym K, Bothe G, Bruschi CV,**
855 **Collins M, Cadag E, Ciarloni L, Clayton C, Coulson RM, Cronin A, Cruz AK, Davies**
856 **RM, De Gaudenzi J, Dobson DE, Duesterhoeft A, Fazelina G, Fosker N, Frasc AC,**
857 **Fraser A, Fuchs M, Gabel C, Goble A, Goffeau A, Harris D, Hertz-Fowler C,**
858 **Hilbert H, Horn D, Huang Y, Klages S, Knights A, Kube M, Larke N, Litvin L, et al.**
859 2005. The genome of the kinetoplastid parasite, *Leishmania major*. *Science*
860 **309**:436-442.
- 861 66. **Seyed N, Peters NC, Rafati S.** 2018. Translating Observations From
862 Leishmanization Into Non-Living Vaccines: The Potential of Dendritic Cell-Based
863 Vaccination Strategies Against *Leishmania*. *Front Immunol* **9**:1227.
- 864 67. **Singh S.** 2014. Changing trends in the epidemiology, clinical presentation, and
865 diagnosis of *Leishmania*-HIV co-infection in India. *Int J Infect Dis* **29**:103-112.
- 866 68. **Lindoso JA, Cota GF, da Cruz AM, Goto H, Maia-Elkhoury AN, Romero GA, de**
867 **Sousa-Gomes ML, Santos-Oliveira JR, Rabello A.** 2014. Visceral leishmaniasis and
868 HIV coinfection in Latin America. *PLoS Negl Trop Dis* **8**:e3136.
- 869 69. **Monge-Maillo B, Norman FF, Cruz I, Alvar J, Lopez-Velez R.** 2014. Visceral
870 leishmaniasis and HIV coinfection in the Mediterranean region. *PLoS Negl Trop Dis*
871 **8**:e3021.
- 872 70. **Romano A, Carneiro MBH, Doria NA, Roma EH, Ribeiro-Gomes FL, Inbar E, Lee**
873 **SH, Mendez J, Paun A, Sacks DL, Peters NC.** 2017. Divergent roles for
874 Ly6C+CCR2+CX3CR1+ inflammatory monocytes during primary or secondary
875 infection of the skin with the intra-phagosomal pathogen *Leishmania major*. *PLoS*
876 *Pathog* **13**:e1006479.
- 877 71. **Glennie ND, Scott P.** 2016. Memory T cells in cutaneous leishmaniasis. *Cell*
878 *Immunol* **309**:50-54.
- 879 72. **Glennie ND, Yeramilli VA, Beiting DP, Volk SW, Weaver CT, Scott P.** 2015. Skin-
880 resident memory CD4+ T cells enhance protection against *Leishmania major*
881 infection. *J Exp Med* **212**:1405-1414.
- 882 73. **Julia V, Glaichenhaus N.** 1999. CD4(+) T cells which react to the *Leishmania major*
883 LACK antigen rapidly secrete interleukin-4 and are detrimental to the host in
884 resistant B10.D2 mice. *Infect Immun* **67**:3641-3644.
- 885 74. **Mazumder S, Maji M, Das A, Ali N.** 2011. Potency, efficacy and durability of
886 DNA/DNA, DNA/protein and protein/protein based vaccination using gp63 against
887 *Leishmania donovani* in BALB/c mice. *PLoS One* **6**:e14644.

- 888 75. **Mazumder S, Maji M, Ali N.** 2011. Potentiating effects of MPL on DSPC bearing
889 cationic liposomes promote recombinant GP63 vaccine efficacy: high
890 immunogenicity and protection. *PLoS Negl Trop Dis* **5**:e1429.
- 891 76. **Bhowmick S, Ravindran R, Ali N.** 2008. gp63 in stable cationic liposomes confers
892 sustained vaccine immunity to susceptible BALB/c mice infected with *Leishmania*
893 *donovani*. *Infect Immun* **76**:1003-1015.
- 894 77. **Sachdeva R, Banerjea AC, Malla N, Dubey ML.** 2009. Immunogenicity and efficacy
895 of single antigen Gp63, polytope and polytopeHSP70 DNA vaccines against visceral
896 Leishmaniasis in experimental mouse model. *PLoS One* **4**:e7880.
- 897 78. **von Schillde MA, Hormannsperger G, Weiher M, Alpert CA, Hahne H, Bauerl C,**
898 **van Huynegem K, Steidler L, Hrnecir T, Perez-Martinez G, Kuster B, Haller D.**
899 2012. Lactocepine secreted by *Lactobacillus* exerts anti-inflammatory effects by
900 selectively degrading proinflammatory chemokines. *Cell Host Microbe* **11**:387-396.
- 901 79. **Karlsson C, Eliasson M, Olin AI, Morgelin M, Karlsson A, Malmsten M, Egesten**
902 **A, Frick IM.** 2009. SufA of the opportunistic pathogen *finegoldia magna* modulates
903 actions of the antibacterial chemokine MIG/CXCL9, promoting bacterial survival
904 during epithelial inflammation. *J Biol Chem* **284**:29499-29508.
- 905 80. **Jauregui CE, Wang Q, Wright CJ, Takeuchi H, Uriarte SM, Lamont RJ.** 2013.
906 Suppression of T-cell chemokines by *Porphyromonas gingivalis*. *Infect Immun*
907 **81**:2288-2295.
- 908 81. **Shiraki Y, Ishibashi Y, Hiruma M, Nishikawa A, Ikeda S.** 2008. *Candida albicans*
909 abrogates the expression of interferon-gamma-inducible protein-10 in human
910 keratinocytes. *FEMS Immunol Med Microbiol* **54**:122-128.
- 911 82. **Casrouge A, Decalf J, Ahloulay M, Lababidi C, Mansour H, Vallet-Pichard A,**
912 **Mallet V, Mottez E, Mapes J, Fontanet A, Pol S, Albert ML.** 2011. Evidence for an
913 antagonist form of the chemokine CXCL10 in patients chronically infected with HCV.
914 *J Clin Invest* **121**:308-317.
- 915 83. **Harth-Hertle ML, Scholz BA, Erhard F, Glaser LV, Dolken L, Zimmer R, Kempkes**
916 **B.** 2013. Inactivation of intergenic enhancers by EBNA3A initiates and maintains
917 polycomb signatures across a chromatin domain encoding CXCL10 and CXCL9. *PLoS*
918 *Pathog* **9**:e1003638.
- 919 84. **Bowen JR, Quicke KM, Maddur MS, O'Neal JT, McDonald CE, Fedorova NB, Puri**
920 **V, Shabman RS, Pulendran B, Suthar MS.** 2017. Zika Virus Antagonizes Type I
921 Interferon Responses during Infection of Human Dendritic Cells. *PLoS Pathog*
922 **13**:e1006164.
- 923 85. **Chaudhary V, Yuen KS, Chan JF, Chan CP, Wang PH, Cai JP, Zhang S, Liang M,**
924 **Kok KH, Chan CP, Yuen KY, Jin DY.** 2017. Selective Activation of Type II Interferon
925 Signaling by Zika Virus NS5 Protein. *J Virol* **91**.
- 926 86. **Consortium IH.** 2005. A haplotype map of the human genome. *Nature* **437**:1299-
927 1320.
- 928 87. **Saraiva EM, Pinto-da-Silva LH, Wanderley JL, Bonomo AC, Barcinski MA,**
929 **Moreira ME.** 2005. Flow cytometric assessment of *Leishmania* spp metacyclic
930 differentiation: validation by morphological features and specific markers. *Exp*
931 *Parasitol* **110**:39-47.
- 932 88. **Wang L, Pittman KJ, Barker JR, Salinas RE, Stanaway IB, Williams GD, Carroll**
933 **RJ, Balmat T, Ingham A, Gopalakrishnan AM, Gibbs KD, Antonia AL, e MN,**

- 934 **Heitman J, Lee SC, Jarvik GP, Denny JC, Horner SM, DeLong MR, Valdivia RH,**
935 **Crosslin DR, Ko DC.** 2018. An Atlas of Genetic Variation Linking Pathogen-Induced
936 Cellular Traits to Human Disease. *Cell Host Microbe* **24**:308-323 e306.
- 937 89. **Kozak M.** 1989. The scanning model for translation: an update. *J Cell Biol* **108**:229-
938 241.
- 939 90. **Barash S, Wang W, Shi Y.** 2002. Human secretory signal peptide description by
940 hidden Markov model and generation of a strong artificial signal peptide for
941 secreted protein expression. *Biochem Biophys Res Commun* **294**:835-842.
- 942 91. **Guler-Gane G, Kidd S, Sridharan S, Vaughan TJ, Wilkinson TC, Tigue NJ.** 2016.
943 Overcoming the Refractory Expression of Secreted Recombinant Proteins in
944 Mammalian Cells through Modification of the Signal Peptide and Adjacent Amino
945 Acids. *PLoS One* **11**:e0155340.
- 946 92. **Schlagenhauf E, Etges R, Metcalf P.** 1998. The crystal structure of the Leishmania
947 major surface proteinase leishmanolysin (gp63). *Structure* **6**:1035-1046.
948